Science Bulletin xxx (xxxx) xxx

Contents lists available at ScienceDirect

Science Bulletin

journal homepage: www.elsevier.com/locate/scib

Article

Quantum oscillations in field-induced correlated insulators of a moiré superlattice

Le Liu [a,b], Yanbang Chu [a,b], Guang Yang [a,b], Yalong Yuan [a,b], Fanfan Wu [a,b], Yiru Ji [a,b], Jinpeng Tian [a,b], Rong Yang [a,c], Kenji Watanabe [d], Takashi Taniguchi [e], Gen Long [c], Dongxia Shi [a,b,c], Jianpeng Liu [f,g], Jie Shen [a,b,c], Li Lu [a,b,c], Wei Yang [a,b,c,*], Guangyu Zhang [a,b,c,*]

[a] Beijing National Laboratory for Condensed Matter Physics and Institute of Physics, Chinese Academy of Sciences, Beijing 100190, China
[b] School of Physical Sciences, University of Chinese Academy of Sciences, Beijing 100190, China
[c] Songshan Lake Materials Laboratory, Dongguan 523808, China
[d] Research Center for Functional Materials, National Institute for Materials Science, Tsukuba 305-0044, Japan
[e] International Center for Materials Nanoarchitectonics, National Institute for Materials Science, Tsukuba 305-0044, Japan
[f] School of Physical Sciences and Technology, ShanghaiTech University, Shanghai 200031, China
[g] ShanghaiTech Laboratory for Topological Physics, ShanghaiTech University, Shanghai 200031, China

ARTICLE INFO

Article history:
Received 5 January 2023
Received in revised form 3 April 2023
Accepted 26 April 2023
Available online xxxx

Keywords:
Quantum oscillations
Correlated insulators
Band inversion
Moiré superlattice
Twisted double bilayer grapheme

ABSTRACT

We report an observation of quantum oscillations (QOs) in the correlated insulators with valley anisotropy of twisted double bilayer graphene (TDBG). The anomalous QOs are best captured in the magneto resistivity oscillations of the insulators at $\nu = -2$, with a period of $1/B$ and an oscillation amplitude as high as 150 kΩ. The QOs can survive up to ~10 K, and above 12 K, the insulating behaviors are dominant. The QOs of the insulator are strongly D dependent: the carrier density extracted from the $1/B$ periodicity decreases almost linearly with D from −0.7 to −1.1 V/nm, suggesting a reduced Fermi surface; the effective mass from Lifshitz-Kosevich analysis depends nonlinearly on D, reaching a minimal value of 0.1 m_e at $D = \sim -1.0$ V/nm. Similar observations of QOs are also found at $\nu = 2$, as well as in other devices without graphite gate. We interpret the D sensitive QOs of the correlated insulators in the picture of band inversion. By reconstructing an inverted band model with the measured effective mass and Fermi surface, the density of state at the gap, calculated from thermal broadened Landau levels, agrees qualitatively with the observed QOs in the insulators. While more theoretical understandings are needed in the future to fully account for the anomalous QOs in this moiré system, our study suggests that TDBG is an excellent platform to discover exotic phases where correlation and topology are at play.

1. Introduction

Quantum oscillations (QOs) of conductance are widely observed in mesoscopic devices [1,2]. For metals in a magnetic field (B), QOs are usually revealed in the Shubnikov-de Haas oscillations (SdHOs) of conductance with a period of $1/B$ due to the Landau quantization of the Fermi surface; for insulators, however, SdHOs are in principle not expected, due to the absence of Fermi surface. Surprisingly, QOs have been observed in Kondo insulators [3–5] (SmB_6 and YbB_{12}), InAs/GaSb quantum wells [6,7], and more recently in the insulating state of WTe_2 [8]. To explain the anomalous QOs, various mechanisms are proposed, including the conventional picture with band inversion, in which the finite density of state (DOS) in the gap oscillates with B due to the broadening of quantized Fermi surfaces away from gaps [9–14], unconventional Landau quantization of neutral Fermions [15–17], and trivial external capacitive mechanism due to the DOS in the gate electrode [18]. However, the strong debates impede the reaching of consensus. Noted that, despite the material differences, these insulators share one common feature, i.e., the insulating gaps are small and resulted from band hybridizations.

Twisted double bilayer graphene (TDBG), a highly tunable moiré flat band system that hosts correlated insulators [19–26], offers another opportunity to unveil the puzzling anomalous QOs. The bands in TDBG [27,28] include flat moiré conduction bands and more dispersive moiré valence band and remote bands, allowing versatile band hybridizations. Besides, perpendicular electrical displacement field (D) could in-situ change the on-site

* Corresponding authors.
E-mail addresses: wei.yang@iphy.ac.cn (W. Yang), gyzhang@iphy.ac.cn (G. Zhang).

https://doi.org/10.1016/j.scib.2023.05.006
2095-9273/

Please cite this article as: L. Liu, Y. Chu, G. Yang et al., Quantum oscillations in field-induced correlated insulators of a moiré superlattice, Science Bulletin, https://doi.org/10.1016/j.scib.2023.05.006

energy between layers and in turn modify nonlinearly the moiré bandwidths as well as the gaps separating different bands [27,29], enabling the facile tuning of Coulomb interactions. Moreover, there is a rich interplay of spin, valley, and Coulomb interaction that results in isospin competition with different polarized ground states of the correlated insulators at half fillings [30–32]. As demonstrated in TDBG [24], it could have a phase transition from metal or spin polarized correlated insulator to valley polarized correlated insulator by increasing D. Thus, TDBG provides a versatile playground for tuning electron correlation and band hybridizations. However, the QOs in the correlated insulators of TDBG as well as other twisted multilayer moiré systems [33–37] have been not explored.

Here, we report an observation of QOs in the correlated insulators of TDBG. We focus on the correlated insulator at $\nu = -2$ in the TDBG device with a graphite gate, and demonstrate the QOs in the insulator from the observation of the resistivity oscillations as a function of $1/B$. Then, we reveal that the insulating QOs are strongly D-field dependent, distinctly different from D insensitive SdHOs of the Bloch electrons in the magnetic field. We also demonstrate the universality of the insulating QOs at $\nu = 2$ as well as in other devices without graphite gate. Lastly, we interpret the D sensitive QOs of the correlated insulators in the picture of band inversion, and we could reproduce a finite DOS in the gap that oscillates with $1/B$ from the calculation of thermal broadened Landau levels (LLs).

2. Materials and methods

The TDBG samples are prepared by using the "cut and stack" method [38], and the details of device information are presented in our previous work [24]. These devices have a dual gate configuration (devices D1, D2 and D3 (D4) with a graphite (Si) bottom gate and gold top gate), which allows independent tuning of the carrier density n and D. Here, $n = (C_{BG}V_{BG} + C_{TG}V_{TG})/e$ and $D = (C_{BG}V_{BG} - C_{TG}V_{TG})/2\varepsilon_0$, where C_{BG} (C_{TG}) is the geometrical capacitance per area for bottom (top) gate, e is the electron charge, and ε_0 is the vacuum permittivity. The filling factor is defined as $\nu = 4n/n_s$, corresponding to the number of carriers per moiré unit cell. Here, n_s is the carrier density to fully fill a moiré band and defined as $n_s = 4/A \approx 8\theta/(\sqrt{3}\,a^2)$, where A is the area of a moiré unit cell, θ is twisted angle, and a is the lattice constant of graphene. In the following, we focus on the magneto transport of the correlated insulators at $\nu = -2$ in device D1 with twisted angle of 1.38°. All measurements are done at $T = 1.8$ K, unless stated otherwise.

3. Results and discussions

3.1. The QOs of the correlated insulators at $\nu = -2$

Fig. 1a–c shows a color mapping of longitudinal resistance $R_{xx}(\nu, D)$ at $B = 0$, 3 and 9 T, respectively. The correlated insulator at $\nu = -2$ develops at finite magnetic field due to orbital Zeeman effect [24]. It shows a periodic oscillating behavior with D at $B = 3$ T in Fig. 1b. This pattern is similar to the LL crossings in layer-polarized systems [39,40], where D tunes the band alignment and further leads to conductance oscillations. Unlike the decoupled cases [39,40] for metals near the band edge, however, the oscillations in Fig. 1b occurs in an insulator when moiré valence bands are half filled. Considering the valley degree of freedom in TDBG, there might be a complicated band structure with multiple Fermi surfaces at $\nu = -2$. At $B = 9$ T in Fig. 1c, the periodic oscillating behavior disappears and only the insulating state remains. To capture the evolution of band structure in magnetic field, we present a Landau fan diagram at $D^* = -0.94$ V/nm (Fig. 1d). LLs are observed fanning out from $\nu = -2$ with $\nu_{LL} = \pm1, \pm2, \pm3, \pm4, \pm5, \pm6$, indicating the presence of both electron-like and hole-like Fermi surfaces and a fully lifted degeneracy of spin and valley in the moiré valence band at such a high D. The interruption of the LLs at some finite B indicates a change of LL degeneracy, which might be due to LLs crossing from a complicated hybridized band structure. While these observations are in line with the previous report [24], however, the alternating color changes between red and white at $\nu = -2$ in Fig. 1d suggest resistance oscillations as a function of B.

The unexpected QOs are better presented in the plot of $R_{xx}(B)$ in Fig. 1e, with a nontrivial oscillation amplitude as high as 150 kΩ at around 6 T. The resistance oscillates periodically with $1/B$, as shown in Fig. 1f. By tracing the position of oscillation peaks and valleys, we obtain a frequency of $B_f \sim 13.3$ T. Here, the frequency can be related to a carrier density via $B_f = n\Phi_0/s$ with s the degeneracy. These oscillations are very sensitive to the temperature, and they are barely visible at $T = 13$ K as shown in Fig. 2a. A full temperature dependence of the oscillations at $\nu = -2$ is depicted in Fig. 2b, where the negative and the positive sign of dR/dT indicate insulator (blue) and metal (red), respectively. The metal insulator transition induced by orbital Zeeman effect occurs at $B \sim 1.2$ T (Fig. 2c) and then the QOs emerge in the insulating regime. Details of the insulating behavior for the QOs at $\nu = -2$ are revealed in the resistivity plots at different temperature in Figs. S1 and S2 (online). In addition, evidence of the bulk insulating behavior at $\nu = -2$ is also revealed in the antiphase oscillations [7] of conductance σ_{xx} and resistivity ρ_{xx} (Fig. 2d) and $\sigma_{xy} \sim 0$ in correlated insulating regions (Fig. S3 online); for comparison, the conventional SdHOs from metallic states at $\nu = -0.32$ shows in phase oscillations (Fig. S4 online). Furthermore, the two terminal resistance transport measurements with edge grounded also suggests the QOs are originated from the insulating bulk states rather than edge states (Fig. S5 online). Thus, the observation of resistance oscillations at $\nu = -2$ is indeed a manifestation of QOs in insulator, distinct from SdHOs in metals.

3.2. The D dependence of insulating QOs

The resistive QOs of the insulator at $\nu = -2$ are observed over a wide range of $|D| > 0.6$ V/nm, as shown in the color mapping of $R_{xx}(D, B)$ at $T = 100$ mK (Fig. 3a). In particular, these QOs emerge as a series of fans at $|D|$ from 0.7 to 1.1 V/nm, which is reminiscent of the Landau fan diagram with varied carrier density. By performing the fast Fourier transform (FFT) of Fig. 3a, the periodicity of these QOs, B_f, scales linearly to the change of D, indicated by the orange dashed line in Fig. 3b. Lastly, the QOs are vanishing at around $|D| \sim 1.17$ V/nm and then reentrant up on further increasing the $|D| > 1.2$ V/nm; however, the oscillating pattern at $|D| > 1.2$ V/nm is seemly antisymmetric compared to those at $|D| < 1.2$ V/nm, suggesting a pi phase change.

The observed D-field dependent resistive QOs at $\nu = -2$ are not due to the Brown-Zak oscillations [41] (BZOs, a feature of the Hofstadter butterfly). The BZOs are observed at a lower displacement field ($|D| < 0.6$ V/nm) in Fig. 3a with low resistance. Distinct from the QOs at $\nu = -2$ that strongly depends on D, the metallic BZOs frequency of $B_f = \sim 46$ T is independent on D (right panel in Fig. 3b), corresponding to the commensuration of $\Phi/\Phi_0 = 1$ for moiré superlattices with a twisted angle of 1.38°. Such BZOs are also observed in the remote valance band ($\nu < -4$) at a high $|D|$ of 0.94 V/nm (Fig. S6 online), where the distinction between the resistive QOs at $\nu = -2$ and the metallic BZOs are demonstrated in their frequency difference. In addition, the insulating QOs at $\nu = -2$ are also not related to the crossing of LLs from $\nu = 0$ and that from $\nu = -4$. Since the latter means that the oscillation period could be traced back to a specific carrier density, i.e., a fixed frequency B_f, regardless of D. However, the observed B_f at $\nu = -2$ is almost

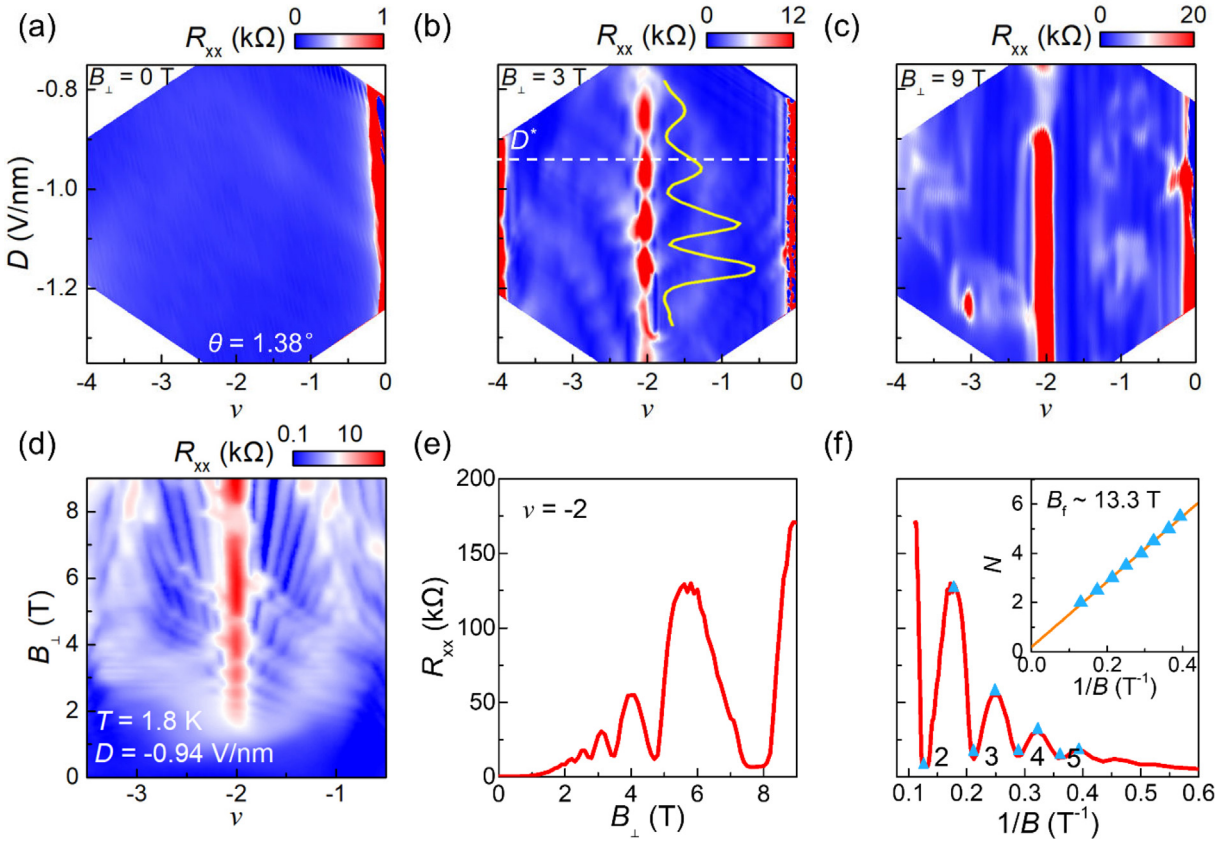

Fig. 1. (Color online) Quantum oscillations of $\nu = -2$ insulators. (a–c) R_{xx} as a function of ν and D at $B_\perp$ = 0, 3 and 9 T, respectively. The yellow line in (b) is a line cut along $\nu = -2$. (d) Landau fan diagram at $D = -0.94$ V/nm and T = 1.8 K. (e) Line cuts at $\nu = -2$ shown in (d). (f) R_{xx} versus $1/B$ at $\nu = -2$. Inset, oscillation index versus $1/B$. Blue triangles correspond to the position of oscillation peak and valley. The orange line corresponds to the linear fitting.

linearly dependent with D, which cannot be explained in the picture of LLs crossings from the CNP and the full filling.

Note that the QOs of the insulator at $\nu = -2$ have also been observed in other three devices, D2 of θ = 1.21° (Fig. S7 online) and D3 of θ = 1.51° (Fig. S8 online) with a metal top gate and a graphite back gate, and D4 with θ = 1.26° (Fig. S9 online) with a metal top gate and a heavy doped Si back gate. Similar to D1, the resistive QOs and the D tunable low oscillation frequency (B_f < 25 T) are different from the BZOs. The observations in both graphite and non-graphite gate devices indicate that the resistive QOs cannot be induced by capacitive mechanism [18] of graphite DOS at high magnetic fields. Besides, we observe the similar QOs of the insulator at ν = 2 in Fig. S10 (online). These observations indicate that the QOs at half fillings are universal for correlated insulators with valley anisotropy where a general model might apply.

3.3. Calculated DOS in an inverted band model

In the following, we interpret the insulating QO at $\nu = -2$ in the picture of band inversion [9–14]. The center idea is to consider the thermal broadening of the LLs from inverted bands, and it will predict a finite DOS in the gap that oscillates with $1/B$, with the B_f defined by the enclosed area of inverted bands without hybridization. Here, the assumption of band inversion at the correlated insulator is motivated from the single-particle band structure calculation in Fig. S11a (online) and Hartree-Fock calculation of the ground states in TDBG [24]. In the continuum model, the finite D breaks C_2 symmetry, which leads to the inequivalence of k and k' points in moiré Brillouin zone. The two bands from K and K' valley constitute an inverted band at these two points due to the time reversal symmetry. Furthermore, this inverted band could evolve from overlapped bands to gapped bands with the hybridization between two valley subbands (partially valley polarized with intervalley coherence). The potential energy difference between two valley subbands K and K' is the sum of the orbital Zeeman effect and Coulomb interaction, described by the formula $\Delta E = 2g\mu_B B + E_c$, where g, μ_B, and E_c are effective g factor, Bohr magneton, and Coulomb interaction energy, respectively. Since the QOs onset at a low magnetic field of ~1.5 T, and the corresponding Zeeman splitting energy should be much smaller than the bandwidth of the two subbands. We further assume that the overlap of the two subbands are determined by E_c. This assumption is supported by the fact that the observed B_f from QOs at $\nu = -2$ is independent of B. Note that the overlap is linearly dependent on D in Fig. 3b. The observation indicates that E_c scales linearly with D, in agreement with the D dependent bandwidth of the moiré valance in Fig. S11b (online).

By doing quantitively analysis, we obtain effective mass m^* and oscillating carrier density n from QOs of the insulator. As shown in Fig. 3c, similar to the SdHOs in metals, the temperature dependence of QOs in the insulator are found following the Lifshitz–Kosevich formula: $\Delta R = R_{xx}(T) - R_{xx}(T = 13\ \mathrm{K}) \sim kT/\sinh(kT)$, where $k = 2\pi^2 k_B m^*/(heB)$. Here, k_B, m^*, h, and e are Boltzmann constant, effective mass, reduced Planck constant, and electron charge, respectively. The obtained m^* from QOs of the insulator varies from 0.1 to 0.15 m_e (m_e is electron mass) in the oscillation region, decreasing with the increase of $|D|$ at first and then rising rapidly after reaching the minimum value close to $D = -1$ V/nm, as shown in Fig. 3d. In the same way, we obtain m^* in Fig. S12 (online) for both the SdHOs and the insulating QOs at $D = -0.94$ V/nm. In

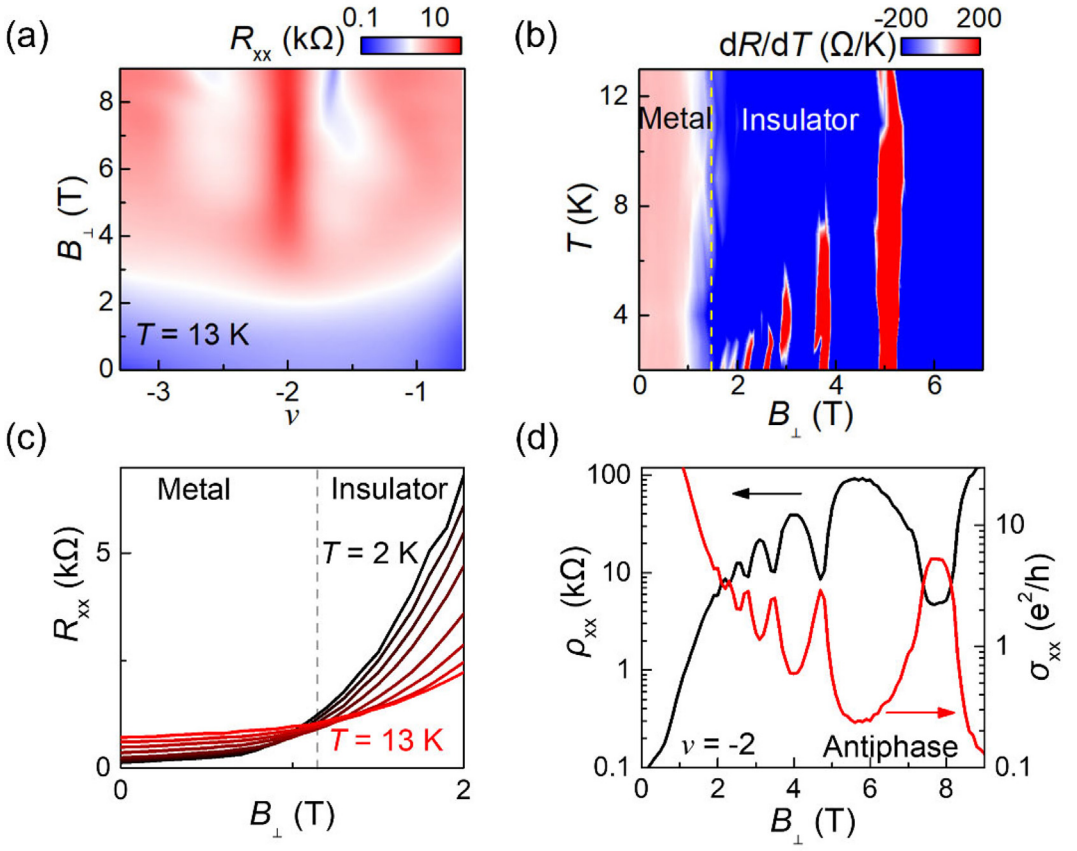

Fig. 2. (Color online) Temperature-dependent quantum oscillations. (a) Landau fan diagram at $D = -0.94$ V/nm and $T = 13$ K. (b) First order derivative of $R_{xx}(T)$ as a function of $B_\perp$ and T at $\nu = -2$. (c) Linecuts of $R_{xx}(B)$ at different temperature. (d) ρ_{xx} and σ_{xx} as a function of $B_\perp$ at $\nu = -2$.

addition, the extracted oscillating carrier density n is shown as an orange line in Fig. 3d, via $B_f = A\Phi_0/(2\pi)^2 = n\Phi_0/s$, where A is the enclosed area of inverted bands without hybridization [11] and $s = 2$ is the spin degeneracy of valley subbands.

Then, we calculate the LLs spectra of the inverted bands at $\nu = -2$, by considering the thermal broadening and the experimental values of gap size Δ, m^*, and oscillating carrier density n. Fig. 4a shows a reconstructed band structure of the moiré valence band at $D = -0.94$ V/nm, with $m_K = 0.15\ m_e$ and $m_{K'} = m_K/0.8$, $\Delta \sim 1.6$ meV, $n \sim 6.5 \times 10^{11}$ /cm^2. The resulted LLs spectrum with inverted bands at $T = 2$ K are shown in top panel of Fig. 4b. The finite low energy DOS in the gap oscillate with $1/B$, which agrees with our experimental data in bottom panel of Fig. 4b. Moreover, the model establishes a close relationship between the size of the enclosed Fermi surface and D, as the latter governs the size of band overlap $\delta\mu$ (details in the Supplementary materials Note 5). The resulted calculations in Fig. 4c indeed predict a change of QOs periodicity as a function of $|D|$, in good agreement with our observation in Fig. 3a. Last but not least, we further carry out numerical calculations to show the LL spectra away from $\nu = -2$, as shown in the comparison between experimental data of longitudinal conductivity and the calculated DOS in Fig. S13 (online). The inverted band model predicts LL intersections away from $\nu = -2$, which qualitatively matches pretty well with experimental crossing points, indicated by the red circles. The agreement between experimental data and the theoretical model further supports our interpretation.

3.4. Discussions

While the model can well explain the data at $|D|$ from 0.7 to 1.1 V/nm, it fails to account for the observations at $|D| \geq \sim 1.2$ V/nm. This discrepancy lies in the over-simplified inverted band model and might suggest a more complicated band structure when Coulomb interaction plays an important role. Also noted, the real systems might acquire phases as D changes, as shown in Fig. S14 (online); however, phase changes are not included in the inverted band model. Besides, the QOs of insulators are supposed to disappear at ultra-low temperature due to the negligible thermal activation, while we observed robust QOs even at $T = 100$ mK (Fig. 3a and Fig. S15 online). The saturated oscillation amplitude in zero temperature limit is probably ascribed to the lifetime broadening of LLs [13] or formation of excitonic insulating behavior [14].

Lastly, we briefly discuss the other possible interpretation of the neutral Fermi surfaces [15–17]. The correlated insulator with valley anisotropy at half fillings in TDBG, together with trigonal moiré superlattice and spin unpolarized, is a possible system with frustrated magnetic interactions for hosting quantum spin liquid states [42,43]. In this exotic picture, the total resistance is the sum of bosonic charge insulator (non-oscillating) and fermionic spinon (oscillating). To testify the neutral Fermion picture, however, conventional charge transport in our work and others falls short, and experimental techniques that could distinguish the charge transport and spin transport are highly demanded.

4. Conclusion and outlook

To sum up, we have observed anomalous oscillating behaviors in the correlated insulator at $\nu = -2$ in the TDBG, with a period of $1/B$ and an oscillation amplitude as high as 150 kΩ. Such insulating QOs are strongly tunable with respect to the D-field, distinctly

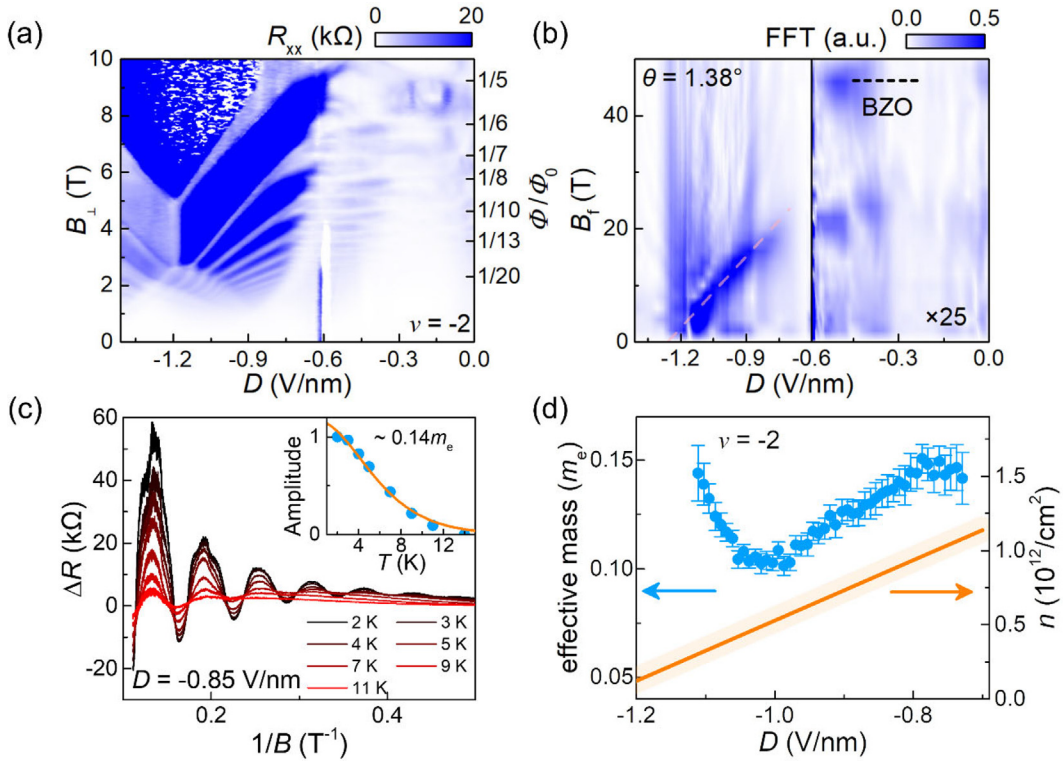

Fig. 3. (Color online) Electric field tunable quantum oscillations. (a) R_{xx} as a function of D and $B_\perp$ at $\nu = -2$ and $T = 100$ mK. (b) FFT of (a). Amplitude is magnified 25 times in a range of $D = 0$ to -0.6 V/nm. the orange dash line is a linear fitting along the amplitude peak. (c) ΔR versus $1/B$ at different temperature. Inset, L-K fitting of the oscillation amplitude. (d) Effective mass and carrier density versus D at $\nu = -2$. Error bars of effective mass are estimated from the least square method. The orange shadow corresponds to the uncertainty of carrier density calculated from FFT results.

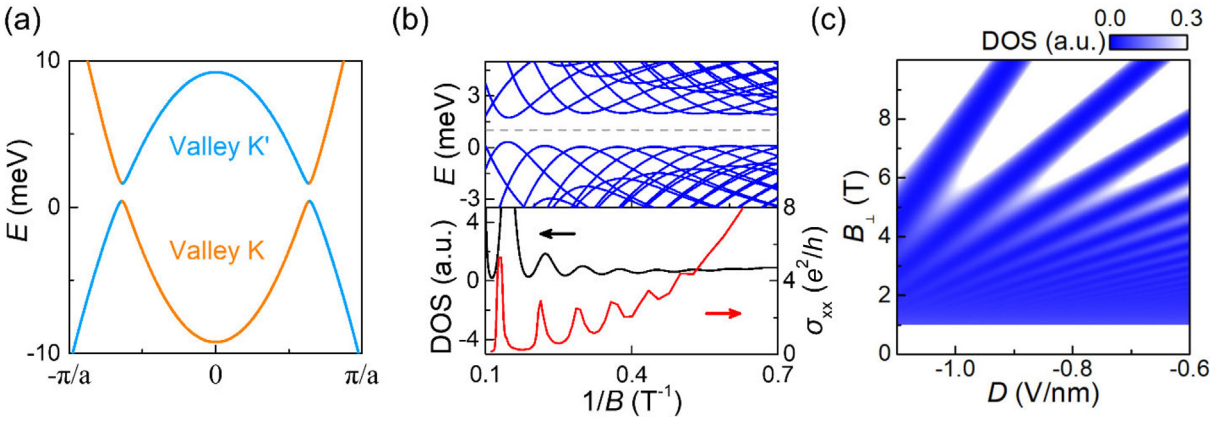

Fig. 4. (Color online) Oscillation in hybridization gaps of inverted band systems. (a) Hybridized inverted Band model. The orange (blue) line corresponds to the energy band in valley K (K'). (b) Top, calculated Landau levels spectrum with $1/B$. The gray line corresponds to the chemical potential. Bottom, calculated low energy DOS in gap (black line) and measured σ_{xx} at $\nu = -2$ and $D = -0.94$ V/nm (red line). (c) Calculated DOS spectrum as a function of D and $B_\perp$.

different from D insensitive SdHOs of the Bloch electrons in the magnetic field. We have also demonstrated the universality of the insulating QOs at $\nu = 2$ as well as in other devices with different twist angles and gate configurations. The observations are captured in the picture of band inversion, which reproduces a finite DOS in the gap that oscillates with $1/B$ from the calculation of thermal broadened LLs. Being an electric field tunable system, TDBG is an excellent platform to study the oscillations in an insulator. The evolution of valley subbands from band inversion to complete separation suggests abundant correlation-driven behaviors and emerging topological phases in field-tunable TDBG systems. While most of the QOs in the correlated insulators are captured in the phenomenological model of the inverted bands with hybridizations, more theoretical and experimental investigations are needed in the future to better understand the insulating QOs in TDBG and other moiré systems as well.

Conflict of interest

The authors declare that they have no conflict of interest.

Acknowledgments

We thank Gang Li, Kun Jiang, Zhida Song, Yuan Wan, and Quansheng Wu for useful discussions. We acknowledge supports from the National Key Research and Development Program

(2020YFA0309600), the National Science Foundation of China (NSFC; 61888102, 11834017, and 1207441), and the Strategic Priority Research Program of Chinese Academy of Sciences (CAS; XDB30000000 and XDB33000000). Measurements at sub-Kelvin temperature are supported by the Synergetic Extreme Condition User Facility at CAS. Gen Long acknowledge the support from NSFC (12104330). Kenji Watanabe and Takashi Taniguchi acknowledge the support from the Elemental Strategy Initiative conducted by the MEXT, Japan (JPMXP0112101001), JSPS KAKENHI (19H05790, 20H00354, and 21H05233) and A3 Foresight by JSPS.

Author contributions

Wei Yang and Guangyu Zhang supervised the project; Wei Yang and Le Liu designed the experiments; Le Liu and Yanbang Chu fabricated the devices and performed the magneto-transport measurement with the assistance of Guang Yang, Jie Shen, Li Lu, Yalong Yuan, FanfanWu, Yiru Ji, Jinpeng Tian, Rong Yang, Gen Long, and Dongxia Shi; Le Liu and Jianpeng Liu calculated the band structure with a continuum model and Landau level DOS in an inverted band model; Kenji Watanabe and Takashi Taniguchi provided hexagonal boron nitride crystals; Wei Yang, Le Liu, and Guangyu Zhang analyzed and interpreted the data; Wei Yang and Le Liu wrote the paper with the input from all the authors.

Data availability

The data that support the findings of this study are available from the corresponding authors upon reasonable request.

Appendix A. Supplementary materials

Supplementary materials to this article can be found online at https://doi.org/10.1016/j.scib.2023.05.006.

References

[1] Shoenberg D. Magnetic oscillations in metals. Cambridge: Cambridge University Press; 1984.
[2] Ihn T. Semiconductor nanostructures: quantum states and electronic transport. New York: Oxford University Press; 2010.
[3] Li G, Xiang Z, Yu F, et al. Two-dimensional fermi surfaces in kondo insulator SmB_6. Science 2014;346:1208–12.
[4] Tan BS, Hsu YT, Zeng B, et al. Unconventional fermi surface in an insulating state. Science 2015;349:287–90.
[5] Xiang Z, Kasahara Y, Asaba T, et al. Quantum oscillations of electrical resistivity in an insulator. Science 2018;362:65–9.
[6] Xiao D, Liu C-X, Samarth N, et al. Anomalous quantum oscillations of interacting electron-hole gases in inverted type-II InAs/GaSb quantum wells. Phys Rev Lett 2019;122:186802.
[7] Han Z, Li T, Zhang L, et al. Anomalous conductance oscillations in the hybridization gap of InAs/GaSb quantum wells. Phys Rev Lett 2019;123:126803.
[8] Wang P, Yu G, Jia Y, et al. Landau quantization and highly mobile fermions in an insulator. Nature 2021;589:225–9.
[9] Pal HK, Piéchon F, Fuchs J-N, et al. Chemical potential asymmetry and quantum oscillations in insulators. Phys Rev B 2016;94:125140.
[10] Knolle J, Cooper NR. Quantum oscillations without a fermi surface and the anomalous de Haas-van Alphen effect. Phys Rev Lett 2015;115:146401.
[11] Zhang L, Song X-Y, Wang F. Quantum oscillation in narrow-gap topological insulators. Phys Rev Lett 2016;116:046404.
[12] Knolle J, Cooper NR. Anomalous de haas-van alphen effect in InAs/GaSb quantum wells. Phys Rev Lett 2017;118:176801.
[13] Shen H, Fu L. Quantum oscillation from in-gap states and a non-hermitian landau level problem. Phys Rev Lett 2018;121:026403.
[14] He W-Y, Lee PA. Quantum oscillation of thermally activated conductivity in a monolayer WTe_2-like excitonic insulator. Phys Rev B 2021;104: L041110. 225.
[15] Motrunich OI. Orbital magnetic field effects in spin liquid with spinon fermi sea: possible application to κ-$(ET)_2Cu_2(CN)_3$. Phys Rev B 2006;73:155115.
[16] Chowdhury D, Sodemann I, Senthil T. Mixed-valence insulators with neutral fermi surfaces. Nat Commun 2018;9:1766.
[17] Sodemann I, Chowdhury D, Senthil T. Quantum oscillations in insulators with neutral fermi surfaces. Phys Rev B 2018;97:045152.
[18] Zhu J, Li T, Young AF, et al. Quantum oscillations in two-dimensional insulators induced by graphite gates. Phys Rev Lett 2021;127:247702.
[19] Shen C, Chu Y, Wu Q, et al. Correlated states in twisted double bilayer graphene. Nat Phys 2020;16:520–5.
[20] Cao Y, Rodan-Legrain D, Rubies-Bigorda O, et al. Tunable correlated states and spin-polarized phases in twisted bilayer-bilayer graphene. Nature 2020;583:215–20.
[21] Liu X, Hao Z, Khalaf E, et al. Tunable spin-polarized correlated states in twisted double bilayer graphene. Nature 2020;583:221–5.
[22] He M, Li Y, Cai J, et al. Symmetry breaking in twisted double bilayer graphene. Nat Phys 2021;17:26–30.
[23] Burg GW, Zhu J, Taniguchi T, et al. Correlated insulating states in twisted double bilayer graphene. Phys Rev Lett 2019;123:197702.
[24] Liu L, Zhang S, Chu Y, et al. Isospin competitions and valley polarized correlated insulators in twisted double bilayer graphene. Nat Commun 2022;13:3292.
[25] Chu Y, Liu L, Shen C, et al. Temperature-linear resistivity in twisted double bilayer graphene. Phys Rev B 2022;106:035107.
[26] He M, Cai J, Zhang Y-H, et al. Chirality-dependent topological states in twisted double bilayer graphene. arXiv: 2109.08255, 2021.
[27] Koshino M. Band structure and topological properties of twisted double bilayer graphene. Phys Rev B 2019;99:235406.
[28] Wu Q, Liu J, Guan Y, et al. Landau levels as a probe for band topology in graphene moiré superlattices. Phys Rev Lett 2021;126:056401.
[29] Chebrolu NR, Chittari BL, Jung J. Flat bands in twisted double bilayer graphene. Phys Rev B 2019;99:235417.
[30] Zhang S, Dai X, Liu J. Spin-polarized nematic order, quantum valley hall states, and field-tunable topological transitions in twisted multilayer graphene systems. Phys Rev Lett 2022;128:026403.
[31] Lee JY, Khalaf E, Liu S, et al. Theory of correlated insulating behaviour and spin-triplet superconductivity in twisted double bilayer graphene. Nat Commun 2019;10:5333.
[32] Liu J, Ma Z, Gao J, et al. Quantum valley hall effect, orbital magnetism, and anomalous hall effect in twisted multilayer graphene systems. Phys Rev X 2019;9:031021.
[33] Cao Y, Fatemi V, Demir A, et al. Correlated insulator behaviour at half-filling in magic-angle graphene superlattices. Nature 2018;556:80–4.
[34] Cao Y, Fatemi V, Fang S, et al. Unconventional superconductivity in magic-angle graphene superlattices. Nature 2018;556:43–50.
[35] Chen G, Sharpe AL, Fox EJ, et al. Tunable correlated chern insulator and ferromagnetism in a moiré superlattice. Nature 2020;579:56–61.
[36] Polshyn H, Zhu J, Kumar MA, et al. Electrical switching of magnetic order in an orbital chern insulator. Nature 2020;588:66–70.
[37] Chen S, He M, Zhang Y-H, et al. Electrically tunable correlated and topological states in twisted monolayer–bilayer graphene. Nat Phys 2021;17:374–80.
[38] Kim K, Yankowitz M, Fallahazad B, et al. Van der waals heterostructures with high accuracy rotational alignment. Nano Lett 2016;16:1989–95.
[39] Sanchez-Yamagishi JD, Taychatanapat T, Watanabe K, et al. Quantum hall effect, screening, and layer-polarized insulating states in twisted bilayer graphene. Phys Rev Lett 2012;108:076601.
[40] Tomić P, Rickhaus P, Garcia-Ruiz A, et al. Scattering between minivalleys in twisted double bilayer graphene. Phys Rev Lett 2022;128:057702.
[41] Krishna Kumar R, Chen X, Auton GH, et al. High-temperature quantum oscillations caused by recurring bloch states in graphene superlattices. Science 2017;357:181–4.
[42] Savary L, Balents L. Quantum spin liquids: a review. Rep Prog Phys 2016;80:016502.
[43] Zhou Y, Kanoda K, Ng T-K. Quantum spin liquid states. Rev Mod Phys 2017;89:025003.

Le Liu received his B.S. degree from Shandong University in 2018. He is currently a Ph.D. candidate at Institute of Physics (IOP), Chinese Academy of Sciences (CAS). His research interest is the cryogenic transport properties of two-dimensional moiré superlattice, such as quantum Hall effect, correlated insulators, ferromagnetism and superconductivity.

Wei Yang received his Ph.D. degree from IOP, CAS in 2014 and then worked as a postdoctoral researcher at École Normale Supérieure in Paris and ICFO-The Institute of Photonic Sciences in Barcelona. He is now an associate professor at IOP, CAS. His research interest lies in exploring the novel phenomena emerging from low dimensional systems including carbon nanotube, 2D materials and moiré superlattices, by quantum transport and high frequency noise thermometry.

Guangyu Zhang received his Ph.D. degree from IOP, CAS in 2004 and then worked as a postdoctoral researcher at Stanford university. He is now a professor at IOP, CAS and deputy director of Songshan Lake Materials Laboratory in Guangdong. His current research interests are low dimensional (especially 2D) materials with focusing on their novel electronic and mechanical properties and related device applications.